

## Band-structure and screening effects on the $KVV$ and $L_{2,3}VV$ Auger spectra of metallic Mg

M. Davies

*Department of Physics, University of Liverpool, Liverpool, United Kingdom L69 3BX*

D. R. Jennison

*Department of Physics, University of Liverpool, Liverpool, United Kingdom L69 3BX  
and Sandia National Laboratories, Albuquerque, New Mexico 87185\**

P. Weightman

*Department of Physics, University of Liverpool, Liverpool, United Kingdom L69 3BX*

(Received 12 January 1984)

The  $KVV$  Auger spectrum of metallic Mg has been obtained with the use of soft-x-ray excitation. The differences between the measured spectral profile and the  $L_{2,3}VV$  profile are found to be explained entirely by the differences in the matrix elements for the two processes. The analysis also suggests that the screening charge induced by the core hole in the Auger initial state is largely  $s$ -like and that other many-body effects play only a minor role in determining the shapes of the Auger lines. It is shown that muffin-tin band-structure calculations may be used for the partial densities of states, provided that their areas are renormalized.

### I. INTRODUCTION

Core-valence-valence (CVV) Auger spectra are interesting because they contain information about the valence electronic structure local to the atom undergoing the core excitation and subsequent Auger decay. This is particularly useful in compounds, alloys, and molecules in which one might wish to examine the valence electronic structure about each different atomic constituent. However, the extraction of this valence information is difficult and it has long been known that CVV profiles cannot be simply interpreted as a convolution of the valence density of electronic states (DOS).<sup>1,2</sup>

Recently, several factors have been studied which affect the CVV spectrum.<sup>3</sup>

(1) *Auger-matrix-element effects:*<sup>4</sup> Because the atomic Auger matrix elements differ for creating valence holes of different angular momenta and because the matrix elements contain wave functions which are highly localized in real space, the valence DOS must be broken into its spectral (i.e.,  $s$ ,  $p$ ,  $d$ , ...) components and within the spirit of a Mulliken population analysis only the local linear combination of atomic orbitals (LCAO) atomic (as opposed to overlap or bonding) charge included in the calculation of Auger amplitudes.

(2) *Initial state core-hole screening:*<sup>5,6</sup> Because the presence of the core hole causes a screening relaxation in which the number of local valence electrons changes (often by the order of unity) and because the relative number of valence electrons of each angular momentum can also change, the Auger profile can be substantially altered from that expected on the basis of the ground-state configuration. For example, in Be metal, the ground-state  $2p:2s$  atomic charge ratio of approximately 2:1 changes to  $\sim 1:1.5$  in the presence of the core hole thus increasing greatly the probability of creating an  $s$ -like valence hole in the final state.

(3) *Final-state hole-hole correlation:*<sup>7-9</sup> In systems in which the two final-state valence holes cannot be effectively screened from each other, usually "filled-band" systems such as oxides, halides, and transition metals such as Ni and Cu, the holes cannot be treated as independent. The latter is the entire basis of the DOS analysis. In these systems localized resonances occur in which the lifetime of two holes upon one site is much longer than normal valence hopping times.

(4) *Nonorthogonality effects:*<sup>6,10</sup> If the Hilbert space spanned by the initial-state-occupied valence orbitals differs substantially from that occupied by ground-state-occupied valence orbitals, many-body effects occur which may be substantial.<sup>6</sup> Schulman and Dow<sup>10</sup> discuss the consequences of nonorthogonality in three parts: shake (the production of three-hole and higher states), Anderson orthogonality, and Friedel replacement transitions. The Schulman and Dow<sup>10</sup> analysis modeled Li metal and found that shake shifts the Auger line shape to lower kinetic energies while the latter effects decrease the Auger amplitude and produce a dominating forward shift, respectively. Schulman and Dow,<sup>10</sup> while defining these factors, did not determine their overall significance since the influences of (1) and (2) above were omitted. One purpose of the present work is to investigate the significance of nonorthogonality in simple metal spectra.

(5) *Effects of collective excitations:* Intrinsic plasmon effects add a low-energy tail to the spectra but have only a minor effect on the major peak.<sup>11</sup>

(6) *Loss:*<sup>12</sup> Since the Auger electron may lose energy (e.g., via extrinsic plasmon effects) while leaving the sample, this also produces a low-energy tail and may distort the main line.

While initially intimidating, this collection of complicating factors are actually quite orderly and logical in their occurrence and should not discourage one from analyzing CVV spectra. For example, in simple metals we

do not expect hole-hole correlation (No. 3) to be at all important or plasmons (No. 5) to appreciably affect the shape of the main line except for the low-energy tail. Studies by Lässer and Fuggle<sup>13</sup> suggest that the screening electron (No. 2) may be assumed to occupy the lowest available atomic orbital. The nonorthogonality effects (No. 4) are difficult to include, but their magnitude may be found by comparing the experimental spectrum with a simple analysis which includes just the Auger matrix element (No. 1) and core-hole screening (No. 2). Loss (No. 6) may be estimated using a backscatter spectrum and may be deconvoluted out of the experimental spectrum if required.<sup>12</sup>

In this paper we investigate two concepts. As mentioned above, Schulman and Dow<sup>10</sup> defined the effects of nonorthogonality within the context of the Li (*KVV*) spectrum. However, Ref. 4 successfully analyzed Li and Jennison *et al.*<sup>5</sup> were quite successful in explaining the Be (*KVV*) spectrum using only matrix-element and core-hole screening concepts. We further test the adequacy of these concepts by performing the first detailed analysis of a second row element, Mg metal, but in addition we analyze both the *KVV* and the *L<sub>2,3</sub>VV* line shapes. Since the Auger matrix elements differ for these decays, the ability to account for differences between these spectra entirely in terms of matrix-element effects argues for an absence of substantial nonorthogonality effects (the latter would presumably be similar for the *KVV* and the *L<sub>2,3</sub>VV* decays since one expects that the initial- and ground-state valence Hilbert spaces would be essentially the same for both decays).

Secondly, the previous analyses<sup>4,5</sup> used density-functional LCAO band-structure calculations to produce a detailed description of the atomic (as opposed to bonding) valence charge. Here we test the idea that one may dispense with this restriction to Auger analysis by using other band-structure results (of the muffin-tin variety) which also provide the angular-momentum-dependent partial DOS (PDOS). We will find that we can use these results providing we renormalize the PDOS areas.

## II. EXPERIMENTAL APPARATUS AND PROCEDURE

Auger spectra were excited using Al *K $\alpha$*  x rays and measured with an AEI ES200 electron spectrometer modified by the addition of a nine channeltron multidetector and a specimen preparation chamber.<sup>14,15</sup> The spectrometer is pumped by ion pumps and titanium sublimation pumps resulting in a base pressure of  $\sim 10^{-10}$  Torr. Specimens were prepared by sputtering Mg onto an Al substrate in an Ar atmosphere of  $\sim 3 \times 10^{-2}$  Torr. After pumping out the Ar, the specimens were transferred to the measuring chamber of the instrument, the pressure in which was at all times  $< 10^{-9}$  Torr. The degree of surface contamination of samples was monitored by measuring the intensities of the carbon and oxygen 1s photoemission peaks relative to the Mg 2s line. Allowing for photoelectron cross sections<sup>16</sup> and escape depths<sup>17</sup> as described earlier<sup>18</sup> we put an upper limit of  $\sim 0.2$  monolayer of oxygen after 3 h. No carbon 1s peak could be resolved with the multidetector after the same interval.

Experimental periods on each sample were therefore limited to  $\sim 2$  h, thereby ensuring a tolerable level of sample contamination.

The region of the Mg spectrum containing the *KVV* Auger spectrum (indicated by the letter A) is shown by the dots in Fig. 1. The two features at  $\sim 1280$  and  $\sim 1290$  eV to low energy are plasmon satellites accompanying the *KVV* transition and the three peaks to high kinetic energy are the sixth, seventh, and eighth plasmon loss satellites associated with the Mg 2s photoelectron line. The ninth plasmon satellite accompanying the Mg 2s line is expected to lie under the Mg *KVV* spectrum but from the trend of decreasing intensity of successive plasmons we expect it to contribute less than  $\sim 8\%$  of the intensity in this region and the feature has been ignored in what follows.

The dots in Fig. 2(a) show the *KVV* spectrum obtained in a total experimental period of 75 h. The instrumental resolution was  $\sim 0.5$  eV.<sup>19</sup> We found the Mg Auger transitions to have *KLL*(<sup>1</sup>*D*<sub>2</sub>):*KL<sub>2,3</sub>V*:*KVV* intensity ratios of  $1.5 \times 10^{-2}$ : $9 \times 10^{-4}$ . In order to estimate the effect on the shape of the *KVV* transition of the plasmon loss and electron scattering contributions, approximations to the latter quantities shown, respectively, by the solid and dashed lines in Fig. 2(a), were subtracted from the observed spectrum to yield the *KVV* Auger profile shown in Fig. 2(b). The procedure for determining these contributions was the same as that applied to the Mg valence band x-ray

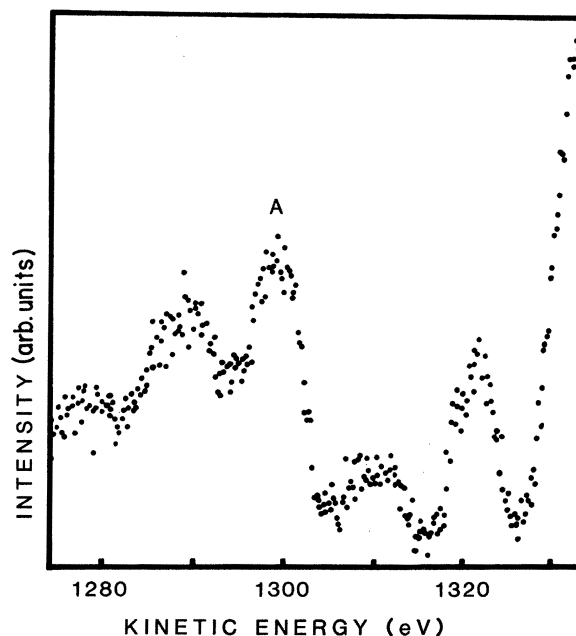


FIG. 1. The region of the Mg photoelectron spectrum containing the *KVV* Auger band spectrum. The *KVV* peak is indicated by the letter A. The two features at  $\sim 1280$  and  $\sim 1290$  eV to low kinetic energy are plasmon satellites accompanying the *KVV* transition while the three peaks to high energy are the sixth, seventh, and eighth plasmon-loss peaks associated with the Mg 2s photoelectron line. The energy scale is referred to the Fermi level.

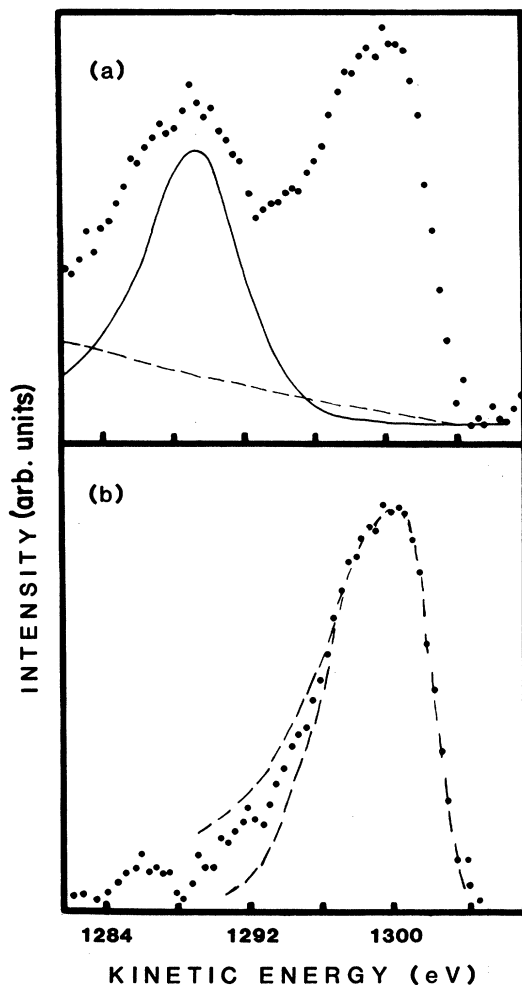


FIG. 2. (a) The background (dashed line) and plasmon (solid line) contributions to the measured  $KVV$  profile (dots). (b) The background and plasmon subtracted  $KVV$  line shape (dots). The dashed lines illustrate the range of possible line shapes obtainable by making different assumptions about the background and plasmon contributions. The energy scale is referred to the Fermi level.

photoelectron spectroscopy (XPS) spectrum<sup>19</sup> and the Mg  $KL_V$  Auger spectrum<sup>20</sup> and is similar to that used by other workers.<sup>13,21</sup> However, such background subtractions are not unique nor rigorously correct<sup>12</sup> and the dashed lines accompanying the dots in Fig. 2(b) show the range of line shapes obtained for different "reasonable" choices of the background contributions. Figure 2(b) shows that the peak position and the shape of the high-energy  $KVV$  edge are independent of the choice of background subtraction.

### III. RESULTS AND DISCUSSION

The dots in Figs. 3(a) and 3(b) show, respectively, the Mg  $KVV$  profile obtained in this work and the  $L_{2,3}VV$  profile measured by Baró and Tagle.<sup>22</sup> The spectra have different profiles and since they involve the same two-hole final states an attempt to reproduce both spectral shapes from calculated Auger matrix elements and  $s$  and  $p$  DOS's is a powerful test of theory.

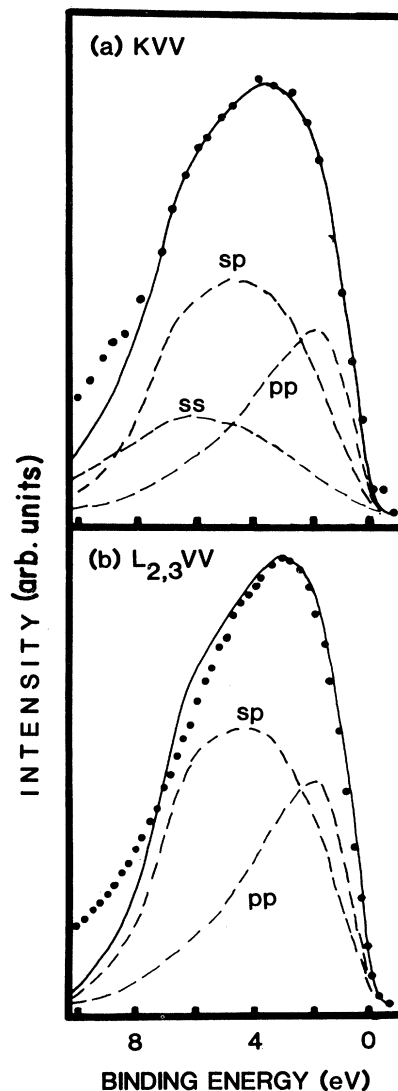


FIG. 3. Comparison of experimental CVV Auger line shapes with those generated by the DOS analysis. The energy scale is referred to the Fermi level,  $E_F$  ( $E_F=0$  eV).

The empirical pseudopotential band-structure calculation of Citrin *et al.*<sup>23</sup> has been shown to yield local partial densities of states in good agreement with XPS and ultraviolet photoelectron spectroscopy (UPS) valence band spectra.<sup>19</sup> Citrin *et al.*<sup>23</sup> were interested in comparing their band-structure calculations with x-ray band spectra so the partial densities of states were determined by projecting out the angular momentum character of their pseudopotential wave functions using a cutoff radius of 1 a.u. The total density of states of Mg metal predicted by the calculation of Citrin *et al.*<sup>23</sup> is then decomposed as shown in Fig. 4.

We now face the problem of converting the published muffin-tin band-structure results, whose PDOS are dependent on just how one analyzes the total charge density into components, into a usable form. We first make use of the fact that only the local atomic charge contributes to the Auger amplitude. Thus, if it were possible to project the muffin-tin Bloch functions onto a minimum basis-set

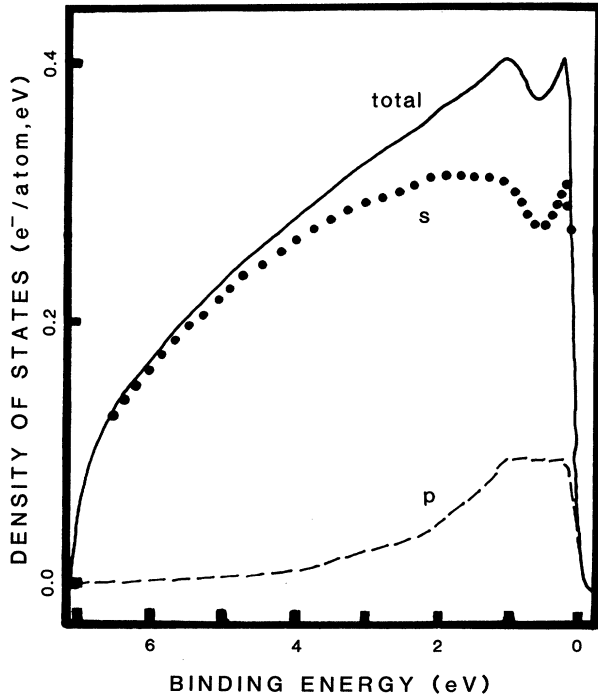


FIG. 4. The density-of-states calculation of Citrin *et al.* (Ref. 23). The solid line is the total DOS and the decomposition into angular momentum character is indicated below the total.

LCAO representation we could directly calculate the atomic charge in each orbital. However, one would need the numerical Bloch functions to accomplish this, and the problem with the published analyses are that most of the overlap (or bonding) charge, which does *not* contribute to the Auger amplitude, is added to the PDOS because it largely lies in one or another of the touching muffin-tin spheres. The latter fact means that we must renormalize the PDOS areas to eliminate the overlap contribution, which we expect will reduce the *s* PDOS relative to the *p* PDOS since the *s* functions have higher overlap and hence more bonding charge. We now make use of two observations. Upon comparison of the PDOS analyses of Citrin *et al.*<sup>23</sup> and Gupta and Freeman,<sup>24</sup> one observes that the shapes of the PDOS differ little while the relative *s:p* areas differ substantially. Any minor differences which actually occur in the shapes will be washed out by the convolution integral. Secondly, during the LCAO analysis of Be metal,<sup>5</sup> one of us (D.R.J.) observed that the *relative* coefficients of the basis functions of a given angular momentum (*s* or *p*) upon one site changed little from point to point in *k* space, except for the most diffuse functions which contribute negligibly to the Auger amplitude. Thus again one may deduce that the shapes of the PDOS are much more independent of the method of analysis than are the areas. We conclude then that we may use the published PDOS shapes but must renormalize the *s:p* area ratio.

In order to interpret the Auger spectra solely in terms of matrix-element and screening effects using published muffin-tin partial densities of states use was made of the following equation:

$$A_{CVV}(E) = D_s(E) * D_s(E) M_{css}^2 \left[ \frac{C_s R}{C_p} \right]^2 + D_s(E) * D_p(E) M_{csp}^2 \left[ \frac{C_s R}{C_p} \right] + D_p(E) * D_p(E) M_{cpp}^2. \quad (1)$$

Here, \* represents a convolution,  $D_s(E)$  and  $D_p(E)$  are the *s* and *p* PDOS's, respectively, the areas under these curves being normalized to unity.  $R$  is the ground-state atomic *s:p* charge ratio,  $M_{cij}$  is an energy-independent matrix element for the transition which produces holes of angular momenta *i* and *j*, and  $C_s$  and  $C_p$  are factors which allow for screening of the initial-state core hole by the valence electrons.<sup>5</sup> The atomic Auger transition rates for the  $L_{2,3}VV$  and  $KVV$  transitions, given by the square of the matrix elements  $M_{cij}$ , are listed in Table I. These values were generated using the method outlined in detail previously<sup>4</sup> and by using the excited-atom-model concept.

The important point to appreciate about Eq. (1) is that if matrix-element and screening effects alone are able to explain the Mg CVV Auger spectra then the single parameter ( $C_s R / C_p$ ) must be independent of the transition under consideration. The peak positions of the  $KVV$  line shape Fig. 2(b) and the  $L_{2,3}VV$  profile previously obtained by Baró and Tagle<sup>22</sup> were both found to be adequately reproduced by taking the factor ( $C_s R / C_p$ ) to be 1.92 ( $\pm 0.10$ ). The  $L_{2,3}VV$  and  $KVV$  profiles predicted on the basis of Eq. (1) both broadened by a Gaussian function of width 0.5 eV to represent instrumental resolution,<sup>19</sup> are compared with experiment (dots) in Fig. 4. The solid lines show the total simulated profile while the decomposition into orbital angular momentum character of the two final-state valence holes is indicated by the dashed curves. There is a noticeable discrepancy between theory and experiment to the low kinetic energy side of the peak position in both cases. In the case of the  $KVV$  this is probably due to the effects of the approximate background subtraction while in the case of the  $L_{2,3}VV$ , the disparity is likely to be due to the fact that Baró and Tagle<sup>22</sup> did not subtract the effects of plasmon excitation from their presented profile.

The success of the above procedure in accounting for the differences between the  $KVV$  and  $L_{2,3}VV$  shapes suggests that the dominant effects influencing the line shapes in the case of Mg are matrix element and screening effects. Because the amount of ground-state atomic valence charge is not known, it is impossible solely from the experimental parameter ( $C_s R / C_p$ ) to determine the angular

TABLE I. Atomiclike Auger transition rates for Mg ( $\times 10^{-4}$  per atomic unit of time).

CVV transition	$M_{css}^2$	$M_{csp}^2$	$M_{cpp}^2$
$L_{2,3}VV$	$5.1 \times 10^{-4}$	2.5	3.8
$KVV$	$8.1 \times 10^{-3}$	$2.5 \times 10^{-2}$	$3.7 \times 10^{-2}$

momentum character of the screening charge. It is, however, possible to demonstrate that the parameter has a reasonable value. If it is assumed that the ground-state  $s:p$  atomic charge ratio  $R$  has a value of 1.0 (not too different from the conclusions of Gupta and Freeman<sup>24</sup>) then the screening electron must be largely  $s$ -like in order to explain the  $C_s/C_p$  value of  $\sim 1.9$ . In fact, any reasonable assumptions regarding the ground-state  $s:p$  charge ratio leads to the conclusion of  $s$ -wave dominated screening which is in agreement with the earlier conclusions of Lässer and Fuggle<sup>13</sup> based on an analysis of  $KVV$  line shapes and x-ray data.

#### IV. CONCLUSIONS

It has been demonstrated that analysis of CVV Auger profiles in wide band metals such as Mg is possible without recourse to LCAO-type band-structure calculations. Partial densities of states given by muffin-tin band-structure calculations may be used provided the areas under the PDOS curves are normalized.

It has also been shown that differences between the  $L_{2,3}VV$  and the  $KVV$  profiles, at least in the case of Mg, can be accounted for by matrix-element and screening effects alone. We therefore find that the nonorthogonality effects described by Schulman and Dow<sup>10</sup> do not play an important role in the determination of Mg CVV Auger profiles.

Finally we have found from our analysis that if reasonable assumptions are made concerning the ground-state  $s:p$  atomic charge ratio the screening charge induced by the core hole in the initial state of the Auger process is largely  $s$ -like, a conclusion which is in agreement with the earlier work of Lässer and Fuggle.<sup>13</sup>

#### ACKNOWLEDGMENTS

We would like to acknowledge support from the Science and Engineering Research Council of the United Kingdom for D.R.J. This work was done in part at Sandia National Laboratories supported by the U. S. Department of Energy under Contract No. DE-AC04-76DP00789.

\*Permanent address.

<sup>1</sup>J. J. Lander, Phys. Rev. **91**, 1382 (1953).

<sup>2</sup>C. J. Powell, Phys. Rev. Lett. **30**, 1179 (1973).

<sup>3</sup>See review articles by P. Weightman, Rep. Prog. Phys. **45**, 753 (1982) and D. R. Jennison, J. Vac. Sci. Technol. **20**, 548 (1982).

<sup>4</sup>D. R. Jennison, Phys. Rev. B **18**, 6865 (1978).

<sup>5</sup>D. R. Jennison, H. H. Madden, and D. M. Zehner, Phys. Rev. B **21**, 430 (1980).

<sup>6</sup>D. R. Jennison, Phys. Rev. A **23**, 1215 (1981).

<sup>7</sup>M. Cini, Surf. Sci. **87**, 483 (1979), and references therein.

<sup>8</sup>G. A. Sawatzky, Phys. Rev. Lett. **39**, 504 (1977).

<sup>9</sup>G. Treglia, M. C. Desjonqueres, F. Ducastelle, and D. Spanjaard, J. Phys. C **14**, 4347 (1981).

<sup>10</sup>J. N. Schulman and J. D. Dow, Int. J. Quantum Chem. **15**, 437 (1981).

<sup>11</sup>J. Fitchek, R. Patrick, and S. M. Bose, Phys. Rev. B **26**, 6390 (1982).

<sup>12</sup>H. H. Madden and J. E. Houston, J. Appl. Phys. **47**, 3071 (1976).

<sup>13</sup>R. Lässer and J. C. Fuggle, Phys. Rev. B **22**, 2637 (1980).

<sup>14</sup>P. Weightman and P. T. Andrews, J. Phys. C **13**, 3529 (1980).

<sup>15</sup>I. R. Holton, P. Weightman, and P. T. Andrews, J. Electron Spectrosc. Relat. Phenom. **21**, 219 (1980).

<sup>16</sup>J. H. Scofield, J. Electron Spectrosc. Relat. Phenom. **8**, 129 (1976).

<sup>17</sup>D. R. Penn, J. Electron Spectrosc. Relat. Phenom. **9**, 29 (1976).

<sup>18</sup>J. F. McGilp, P. Weightman, and E. J. McGuire, J. Phys. C **10**, 3445 (1977).

<sup>19</sup>M. Davies, P. H. Hannah, P. Weightman, and P. T. Andrews, J. Phys. F (to be published).

<sup>20</sup>M. Davies, D. R. Jennison, and P. Weightman, J. Phys. C **17**, L107 (1984).

<sup>21</sup>P. M. Th. M. Van Attekum and J. M. Trooster, J. Phys. F **8**, L169 (1978).

<sup>22</sup>A. M. Baró and J. A. Tagle, J. Phys. F **8**, 563 (1978).

<sup>23</sup>P. H. Citrin, G. K. Wertheim, and M. Schlüter, Phys. Rev. B **20**, 3067 (1979).

<sup>24</sup>R. P. Gupta and A. J. Freeman, Phys. Rev. Lett. **36**, 1194 (1976).